

Multiscale Analysis of Heart Rate Variability: A Comparison of Different Complexity Measures

JING HU,^{1,2} JIANBO GAO,¹ WEN-WEN TUNG,³ and YINHE CAO⁴

¹PMB Intelligence LLC, P.O. Box 2077, West Lafayette, IN 47996, USA; ²Affymetrix, Inc., 3380 Central Expressway, Santa Clara, CA 95051, USA; ³Department of Earth and Atmospheric Sciences, Purdue University, West Lafayette, IN 47907, USA; and ⁴BioSieve, 1026 Springfield Drive, Campbell, CA 95008, USA

(Received 28 March 2009; accepted 26 November 2009; published online 12 December 2009)

Abstract—Heart rate variability (HRV) is an important dynamical variable of the cardiovascular function. There have been numerous efforts to determine whether HRV dynamics are chaotic or random, and whether certain complexity measures are capable of distinguishing healthy subjects from patients with certain cardiac disease. In this study, we employ a new multiscale complexity measure, the scale-dependent Lyapunov exponent (SDLE), to characterize the relative importance of nonlinear, chaotic, and stochastic dynamics in HRV of healthy, congestive heart failure (CHF), and atrial fibrillation subjects. We show that while HRV data of all these three types are mostly stochastic, the stochasticity is different among the three groups. Furthermore, we show that for the purpose of distinguishing healthy subjects from patients with CHF, features derived from SDLE are more effective than other complexity measures such as the Hurst parameter, the sample entropy, and the multiscale entropy.

Keywords—Heart rate variability, Cardiovascular system, Multiscale analysis, Scale-dependent Lyapunov exponent.

INTRODUCTION

A cardiovascular system, being comprised of multiple subsystems with complicated nonlinear interactions, is an outstanding example of multiscale systems. An important dynamical variable of the cardiovascular system is the heart rate variability (HRV), which refers to the beat-to-beat alterations in heart rate. The most salient feature of HRV is its spontaneous fluctuation, even if the environmental parameters are maintained constant and no perturbing influences can be identified. This is evident in Fig. 1, where the RR intervals of a normal young subject are shown. RR interval is the time duration between two consecutive R waves in the electrocardiogram (ECG). We observe from Fig. 1 that

the RR interval data are highly nonstationary (in the sense that the mean, variance, and other statistical moments vary with time) and multiscaled, appearing oscillatory for some period of time (Figs. 1b and 1d), and then varying as a type of $1/f$ process whose power-spectral-density (PSD) decays in a power law fashion (Figs. 1c and 1e).

Since the observation that HRV is affected by various cardiovascular disorders, many methods have been proposed to analyze it. They include time domain and frequency domain based methods (see Task Force of the European Society of Cardiology and the North American Society of Pacing & Electrophysiology,³² and references therein), as well as methods derived from chaos and random fractal theory.^{1–3,18–21,23–28,30,34} Much of these efforts have been focused on determining whether HRV dynamics are chaotic or random, and whether certain complexity measures can effectively distinguish healthy subjects from patients with certain cardiac disease. To shed new light on these problems, we employ a new multiscale complexity measure, the scale-dependent Lyapunov exponent (SDLE),^{4,7} to carry out a multiscale analysis of HRV of three types of subjects: normal, congestive heart failure (CHF), and atrial fibrillation (AF). We shall further compare SDLE with other complexity measures in terms of how well the metrics can be used to distinguish healthy subjects from patients with CHF.

The remainder of the paper is organized as follows. In “[SDLE as a Multiscale Complexity Measure](#)” section, we briefly describe the SDLE, focusing on its properties that are most relevant to HRV analysis. In “[HRV Analysis by SDLE](#)” section, we use the SDLE to analyze HRV, and consider how to distinguish healthy subjects from patients with CHF. In “[Distinguishing Healthy Subjects from Patients with CHF Using Other Complexity Measures](#),” we analyze HRV using other complexity measures and compare their performance in

Address correspondence to Jianbo Gao, PMB Intelligence LLC, P.O. Box 2077, West Lafayette, IN 47996, USA. Electronic mail: jing.hu@gmail.com, jbgao@pmbintelligence.com

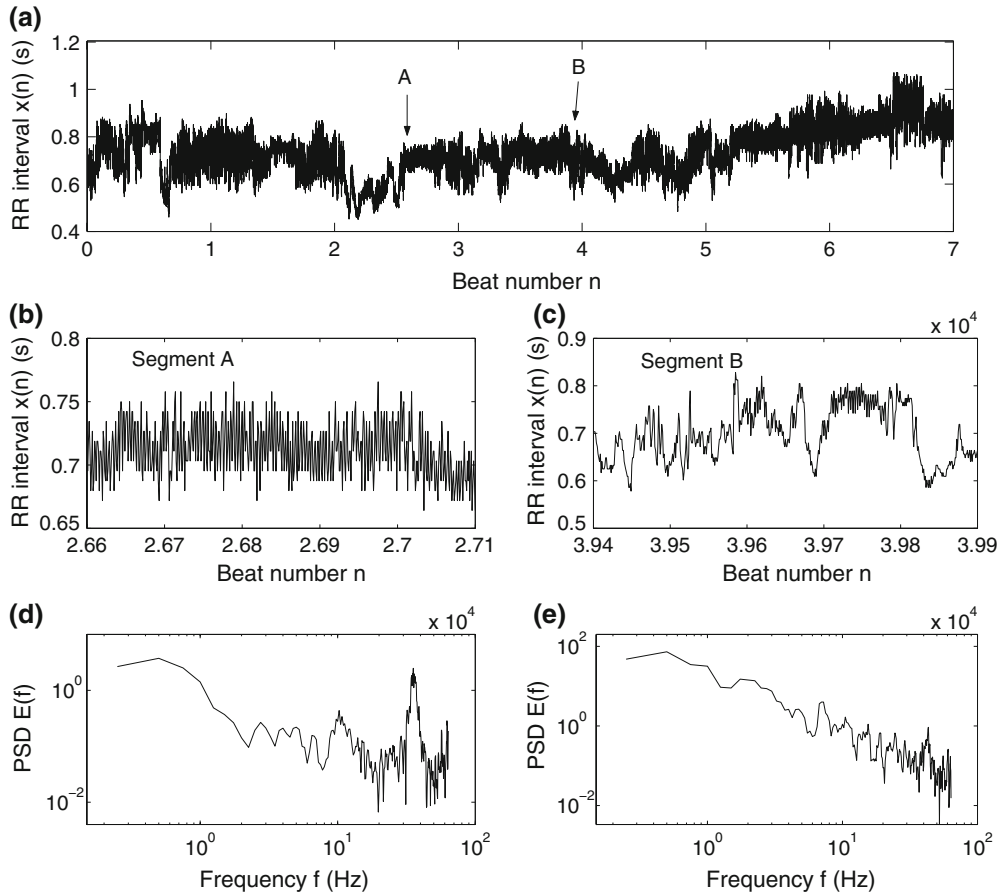


FIGURE 1. (a) The HRV data for a normal subject; (b, c) the segments of signals indicated as A and B in (a); (d, e) power spectral density (PSD) for the signals shown in (b, c).

distinguishing healthy subjects from patients with CHF with that based on the SDLE. In “[Concluding Discussions](#),” we make a few concluding remarks.

SDLE AS A MULTISCALE COMPLEXITY MEASURE

SDLE is defined in a phase space through consideration of an ensemble of trajectories.^{4,7} In the case of a scalar time series $x(1), x(2), \dots, x(n)$, a suitable phase space may be obtained by using time delay embedding^{22,29,31} to construct vectors of the form:

$$V_i = [x(i), x(i+L), \dots, x(i+(m-1)L)], \quad (1)$$

where m and L are called the embedding dimension and the delay time, respectively. For chaotic systems, m and L have to be chosen according to certain optimization criterion.⁴ For a stochastic process, which is infinite-dimensional, the embedding procedure transforms a self-affine stochastic process to a self-similar process in a phase space, and often $m = 2$ is not only

sufficient, but also best illustrates a nonchaotic scaling behavior from a finite dataset.^{4,7}

We now be more concrete. Denote the initial distance between two nearby trajectories by ϵ_0 , and their *average distances* at time t and $t + \Delta t$, respectively, by ϵ_t and $\epsilon_{t+\Delta t}$, where Δt is small. The SDLE $\lambda(\epsilon_t)$ is defined by^{4,7}

$$\epsilon_{t+\Delta t} = \epsilon_t e^{\lambda(\epsilon_t)\Delta t}, \quad \text{or} \quad \lambda(\epsilon_t) = \frac{\ln \epsilon_{t+\Delta t} - \ln \epsilon_t}{\Delta t}. \quad (2)$$

Or equivalently by,

$$\frac{d\epsilon_t}{dt} = \lambda(\epsilon_t)\epsilon_t, \quad \text{or} \quad \frac{d \ln \epsilon_t}{dt} = \lambda(\epsilon_t). \quad (3)$$

To compute SDLE, we can start from an arbitrary number of shells,

$$\epsilon_k \leq \|V_i - V_j\| \leq \epsilon_k + \Delta\epsilon_k, \quad k = 1, 2, 3, \dots, \quad (4)$$

where V_i, V_j are reconstructed vectors, ϵ_k (the radius of the shell) and $\Delta\epsilon_k$ (the width of the shell) are arbitrarily chosen small distances ($\Delta\epsilon_k$ is not necessarily a constant). Then, we monitor the evolution of all pairs of

points (V_i, V_j) within a shell and take average. Eq. (2) can now be written as

$$\lambda(\epsilon_t) = \frac{\langle \ln \|V_{i+t+\Delta t} - V_{j+t+\Delta t}\| - \ln \|V_{i+t} - V_{j+t}\| \rangle}{\Delta t}, \tag{5}$$

where t and Δt are integers in unit of the sampling time, and the angle brackets denote average within a shell. Note that this computational procedure is similar to that for computing the so-called time-dependent exponent curves.^{10–12}

Note that the initial set of shells serve as initial values of the scales; through evolution of the dynamics, they will automatically converge to the range of inherent scales that define Eqs. (2) and (3). Also note that when analyzing chaotic time series, the condition

$$|j - i| \geq (m - 1)L \tag{6}$$

needs to be imposed when finding pairs of vectors within a shell, to eliminate the effects of tangential motions.⁴ This condition is often also sufficient for an initial scale to converge to the inherent scales.⁴

To better understand SDLE, it is instructive to point out a relation between SDLE and the largest positive Lyapunov exponent λ_1 for true chaotic signals. It is given by⁴

$$\lambda_1 = \int_0^{\epsilon^*} \lambda(\epsilon) p(\epsilon) d\epsilon, \tag{7}$$

where ϵ^* is a scale parameter (for example, used for re-normalization when using Wolf *et al.*'s algorithm³³), $p(\epsilon)$ is the probability density function for the scale ϵ given by

$$p(\epsilon) = Z \frac{dC(\epsilon)}{d\epsilon}, \tag{8}$$

where Z is a normalization constant satisfying $\int_0^{\epsilon^*} p(\epsilon) d\epsilon = 1$, and $C(\epsilon)$ is the well-known Grassberger–Procaccia's correlation integral.^{14,15}

SDLE has distinctive scaling laws for different types of time series. Those most relevant to HRV analysis are listed here.

1. For clean chaos on small scales, and noisy chaos with weak noise on intermediate scales,

$$\lambda(\epsilon) = \lambda_1. \tag{9}$$

2. For clean chaos on large scales where memory has been lost and for noisy chaos (including noise-induced chaos^{5,6,17}) on small scales,

$$\lambda(\epsilon) \sim -\gamma \ln \epsilon, \tag{10}$$

where $\gamma > 0$ is a parameter. Recently, using an ensemble forecasting approach, we have

proven that $\gamma = D/D(\epsilon_0)$, where D and $D(\epsilon_0)$ are the information dimension on infinitesimal and an initial finite scale in ensemble forecasting.⁹ When a noisy dataset is finite, due to lack of data, D would soon saturate when m exceeds certain value. However, if the finite scale is quite large, $D(\epsilon_0) \sim m$, for a wide range of m . Therefore, $\gamma \sim 1/m$ when m exceeds certain value. The implications of this point to the calculation of SDLE from HRV will be further discussed later.

3. For white noise, when the evolution time $t \leq (m - 1)L$, where $(m - 1)L$ is the embedding window length, we have a scaling described by Eq. (10)^{7,4,13}; when $t > (m - 1)L$,

$$\lambda(\epsilon) \approx 0. \tag{11}$$

Note that noisy chaos usually has the scaling of Eq. (10) on a much longer time scale range, and therefore, noisy chaos is quite different from white noise. Also note that Eq. (7) yields $\lambda_1 > 0$ for white noise, when $t \leq (m - 1)L$ and $\epsilon \ll 1$. This implies that $\lambda_1 > 0$ obtained using Wolf *et al.*'s algorithm^{5,33} is not a sufficient indicator of chaos.

4. For random $1/f^{2H+1}$ processes, where $0 < H < 1$ is called the Hurst parameter which characterizes the correlation structure of the process: depending on whether H is smaller than, equal to, or larger than $1/2$, the process is said to have anti-persistent, short-range, or persistent long-range correlations,^{4,8}

$$\lambda(\epsilon) \sim \epsilon^{-1/H}. \tag{12}$$

Note the standard Brownian motion corresponds to $H = 1/2$, and generally $H < 1/2$ for HRV.^{1,18,23}

To facilitate HRV analysis, we now discuss an important concept, the characteristic scale (or limiting scale), ϵ_∞ , which is defined by the scales where SDLE is close to 0. It is closely related to the total variation or the energy of the signal. For example, for a chaotic system, ϵ_∞ defines the size of the chaotic attractor. If one starts from $\epsilon_0 \ll \epsilon_\infty$, then, regardless of whether the data are deterministically chaotic or simply random, ϵ_t will initially increase with time and gradually settle around ϵ_∞ . Consequentially, $\lambda(\epsilon_t)$ will be positive before ϵ_t reaches ϵ_∞ . On the other hand, if one starts from $\epsilon_0 \gg \epsilon_\infty$, then ϵ_t will simply decrease, yielding negative $\lambda(\epsilon_t)$, again regardless of whether the data are chaotic or random. When $\epsilon_0 \sim \epsilon_\infty$, then $\lambda(\epsilon_t)$ will stay around 0. Note that typically ϵ_∞ is different from the inherent scales mentioned earlier: the latter are the scales that define Eqs. (2) or (3), but not necessarily

imply $\lambda(\epsilon_t) \approx 0$. However, in the case of white noise-like signals, usually the only resolvable scale is the characteristic scale, and therefore, the inherent scales reduce to the characteristic scale. Not only so, the range of the characteristic scale usually will be very narrow. As we will see later, HRV of AF case belongs to such a case.

HRV ANALYSIS BY SDLE

We examine two sets of HRV data downloaded from the PhysioNet, <http://www.physionet.org/physiobank/database/#ecg>. Detailed information on the data analyzed in this study is summarized in Table 1. One set contains 18 healthy subjects and 15 subjects with CHF. The other set contains three types of HRV, normal, CHF, and AF, each with five subjects. The second set is specifically designed for the December 15, 2008 special issue of *Chaos*, entitled *Controversial Topics in Nonlinear Science: Is the Normal Heart Rate Chaotic?* In the following analysis, we used the raw HRV data instead of the data with outliers filtered out. This is because outliers contribute little to the inherent scales in the reconstructed phase space, and therefore do not affect calculation of SDLE. Being able to directly work on raw HRV data without any preprocessing is one of the merits of SDLE.

We have found (and will show momentarily) that HRV data are mostly stochastic, in the sense that the scaling described by Eq. (9) is not observed in any significant scale range in any of the HRV datasets, no matter what embedding parameters are used. The noisy nature of HRV suggests that it is best to construct a phase space with $m = 2$, $L = 1$ when analyzing a finite dataset. Below, we first discuss the general behaviors of SDLE for HRV of the three types of subjects, then summarize the effects of embedding parameters and data length on the behaviors of SDLE.

Figure 2a1 illustrates the scaling of SDLE for HRV of healthy subjects in general. We clearly observe the scaling described by Eq. (10) on the smallest scales.

When Fig. 2a1 is re-plotted in log–log scale, as shown in Fig. 2a2 (see Fig. 3 for an expanded scaling of the linear region), we observe a linear-like relation on larger scales (corresponding to where $\lambda(\epsilon)$ is slightly positive), with a Hurst parameter $H = 1/6.93 \approx 0.14$. Therefore, the dynamics of normal HRV also contain a $1/f$ -like behavior described by the scaling of Eq. (12). Note that the scale-range where Eq. (12) holds is necessary short, since H here is very small.

The behavior of SDLE for HRV of CHF subjects is markedly different from that of normal HRV. A typical result is shown in Fig. 2b1, in semi-log scale. Note that the value of $\lambda(\epsilon)$ is now much closer to zero, and the pattern of $\lambda(\epsilon)$ is somewhat oscillatory. Inability to resolve the dynamics on scales with $\lambda(\epsilon)$ markedly different from zero is a signature of high-dimensional system.⁴ Therefore, the dimension of HRV dynamics in CHF subjects is much higher than that in normal subjects. When Fig. 2b1 is replotted in log–log scale, as shown in Fig. 2b2, an approximate linear relation emerges, almost on all scales. This suggests that HRV in CHF subjects behaves as a $1/f$ process described by Eq. (12). The slope in the figure gives a Hurst parameter $H = 1/5.19 \approx 0.19$. At this point, it should be emphasized that the pattern of SDLE in Figs. 2a2 and 2b2 is quite different from that of fractional Brownian motion (fBm) processes.^{4,7} Two reasons may be that fBm processes are linear, monofractal random processes, while HRV dynamics are nonlinear^{27,34} and multifractal.¹⁸

Finally, we examine SDLE for HRV of AF patients. A representative result is shown in Fig. 2c1 and 2c2, in semi-log and log–log scale, respectively. We only observe $\lambda(\epsilon) \approx 0$. Bear in mind that for white noise, we also only observe $\lambda(\epsilon) \approx 0$ (Eq. 11) when t is larger than the embedding window length. Furthermore, the scale range resolved from HRV of AF patients is much narrower than those for normal and CHF HRVs, indicating that ϵ , defined in an average sense, is always in an equilibrium-like state for HRV of AF subjects. In this case, it is not meaningful to assign a scaling relation for the data. Therefore, the dynamics in HRV of

TABLE 1. A description of the data analyzed in this study.

	Dataset 1		Dataset 2		
	Normal	CHF	Normal	CHF	AF
Number of subjects	18	15	5	5	5
Number of segments analyzed per subject	1	1	1	1	1
Segment analyzed	First 30k points	First 30k points	Whole data	Whole data	Whole data
Sampling frequency (Hz)	128	250	128	250	128
Time duration (h)	~25	~20	~24	~24	~24

The sampling frequency is for the ECG signals where RR intervals were derived.

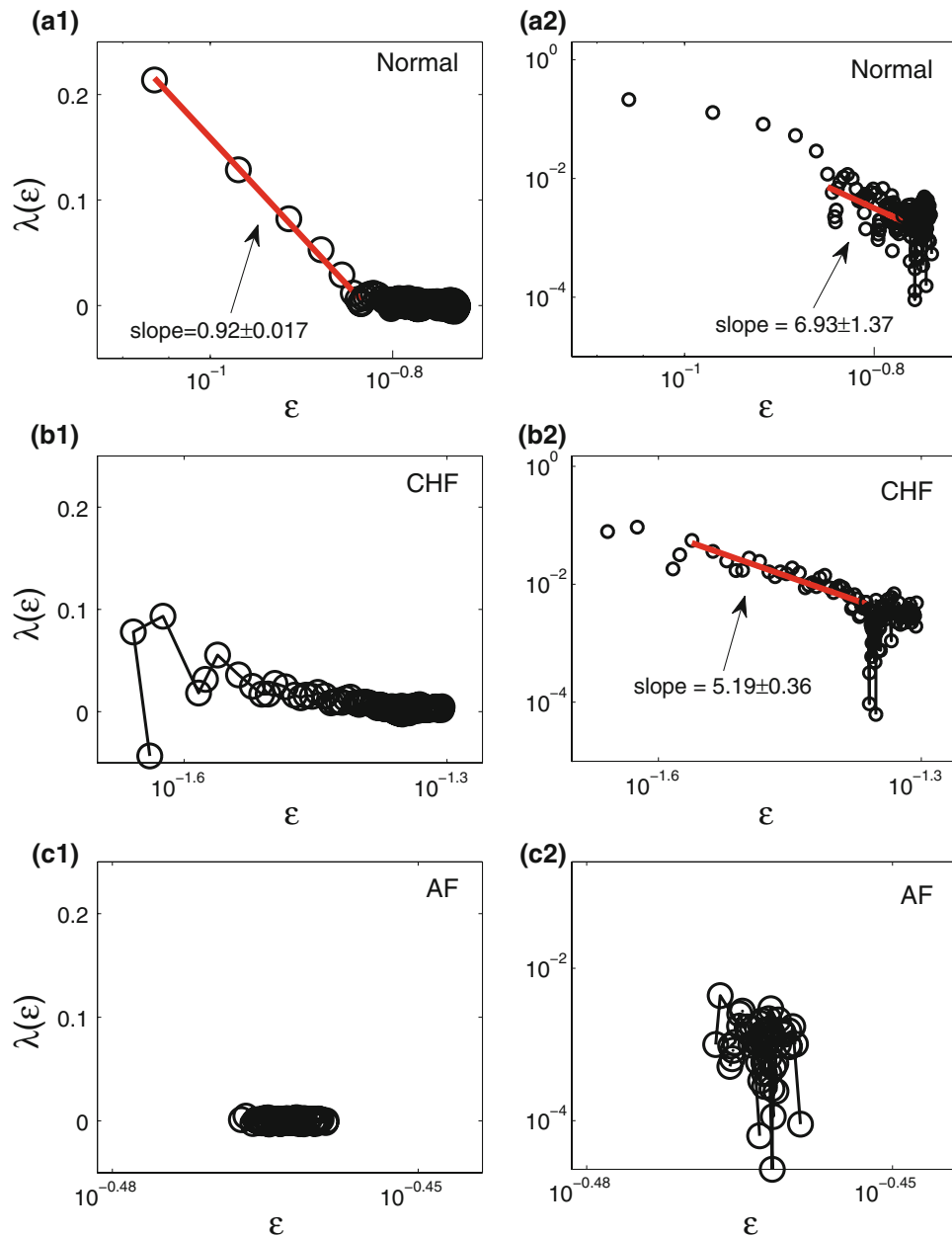


FIGURE 2. $\lambda(\epsilon)$ curves for HRV of (a1, a2) normal, (b1, b2) CHF, and (c1, c2) AF subjects. Plots in the left panel are in semi-log scale, while those in the right panel are in log–log scale. For better comparison, results for datasets n1rr.txt, c1rr.txt, and a3rr.txt are shown here, since they have similar length (99,791, 75,543, and 85,304 points, respectively). The results are similar when only part of these data is used.

AF subjects are like white noise. This suggests that the dimension of HRV of AF subjects is the highest among the three groups.

We now summarize the effects of data length and embedding dimension on calculating SDLE from HRV: (i) With fixed embedding parameters, for a long HRV dataset, SDLE curves corresponding to different shells defined by Eq. (4) often do not collapse on one another, but are parallel; similarly, the scaling of Eq. (10) may shift horizontally when the data length

changes. However, γ remains quite stable. An example is shown in Fig. 4. (ii) For a dataset of finite fixed length, change of the delay time L almost has no effect on the SDLE curve. An example is shown in Fig. 5. (iii) For a dataset of finite fixed length, when the embedding dimension m becomes bigger, the scale range defining the scaling of Eq. (10) becomes shorter; also, as pointed out when discussing Eq. (10), γ is roughly inversely proportional to m when m is large. An example is shown in Fig. 6. (iv) The scaling of

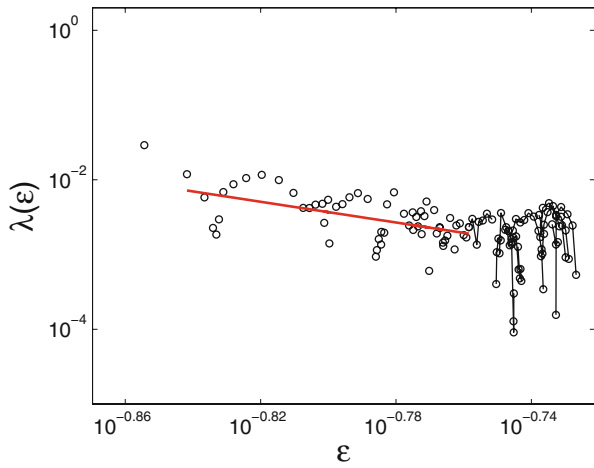


FIGURE 3. The ϵ scaling corresponding to the linear region of Fig. 2(a2) is expanded so that the linear region can be better visualized.

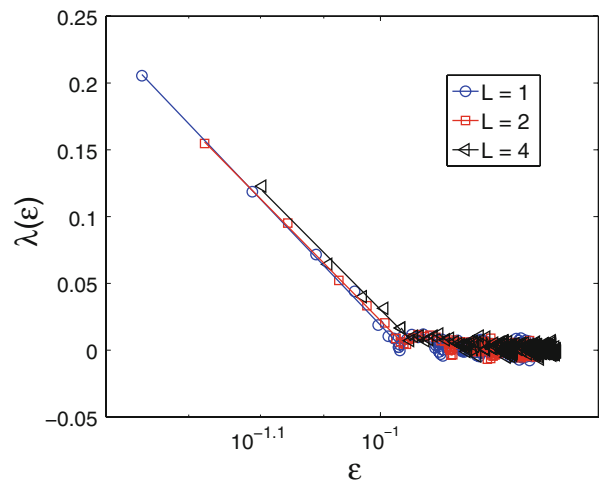


FIGURE 5. The variation of SDLE with delay time L , where a normal HRV dataset of length 10,000 is used. Different L almost does not change the SDLE curves.

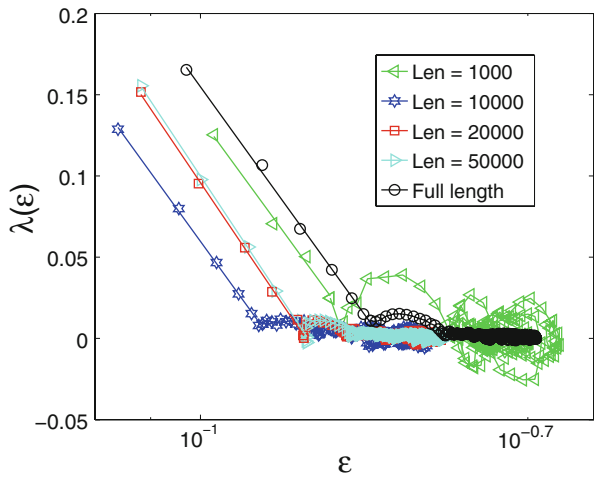


FIGURE 4. The variation of SDLE with data length, where $m = 4$, $L = 1$. Notice the horizontal shifting of the SDLE curves.

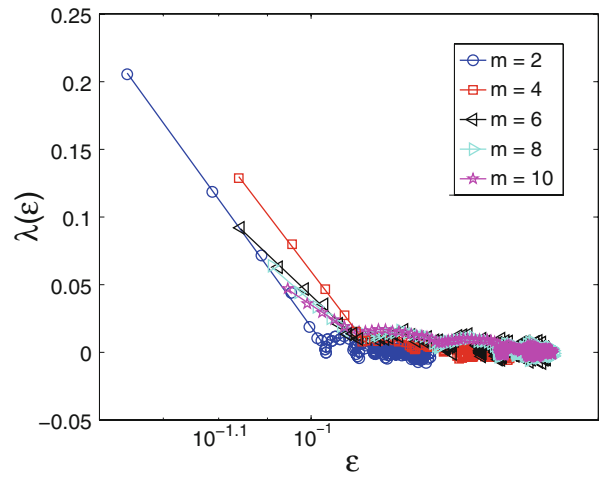


FIGURE 6. The variation of SDLE with m , where a normal HRV dataset of length of 10,000 is used. Note that when $m \geq 4$, $\gamma \sim 1/m$, as expected from our theory.

Eq. (12), while becoming less well defined when a dataset becomes shorter, is independent of the embedding dimension. This is clearly shown in Fig. 7. Logically, this result has to hold; otherwise, H becomes meaningless.

Next, we discuss how to distinguish between healthy subjects and patients with CHF from HRV analysis. For this purpose, we focus on the set of HRV with 18 normal and 15 CHF subjects. Based on Figs. 2a1 and 2b1, we have devised two simple measures, or features. One is to characterize how well the linear relation between $\lambda(\epsilon)$ and $\ln \epsilon$ is defined. We have quantified this by calculating the error between a fitted straight line and the actual $\lambda(\epsilon)$ vs. $\ln \epsilon$ plots of Figs. 2a1 and 2b1. The second feature is

to characterize how well the characteristic scale ϵ_∞ is defined. This is quantified by the ratio between two scale ranges: the first is the scale range where Eq. (10) is defined (roughly, from the second to the sixth point of the $\lambda(\epsilon)$ curves—the first point, corresponding to the embedding window length $(m - 1)L = 1$, is excluded); the second scale range is an estimation of the width of the characteristic scale (to cope with oscillatory behavior in this scale range, we used the 7th to the 11th point of the $\lambda(\epsilon)$ curves). The mean and standard deviation of the first scale range for the normal subjects is 0.1217 and 0.0222, respectively, while the mean and standard deviation of the same scale range for the CHF subjects is 0.0572 and 0.0326, respectively. The mean and standard deviation of the

second scale range for the normal subjects is 0.0143 and 0.010, respectively, while the mean and standard deviation of the same scale range for the CHF

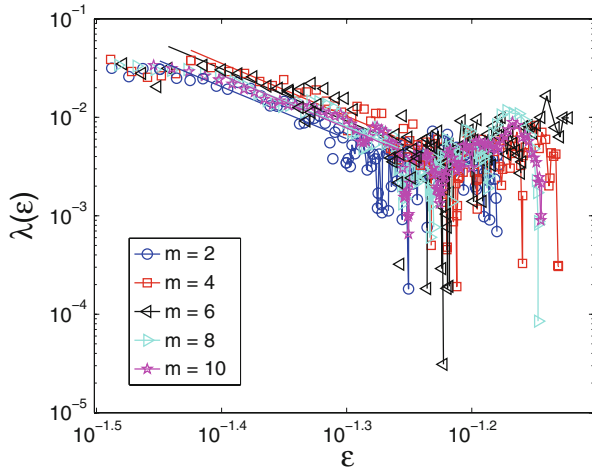


FIGURE 7. Independence of the $1/f$ scaling (Eq. 12) with m , based on a CHF dataset of length 10,000.

subjects is 0.0433 and 0.016, respectively. The receiver operating characteristic (ROC) curves using these two features for distinguishing healthy subjects from patients with CHF are shown in Fig. 8, where true positive rates (TPR) and the false positive rates (FPR) are defined, respectively, as the number of subjects correctly and falsely classified divided by the number of subjects in the corresponding group (either normal or CHF group), when the feature parameter is set at certain threshold value. Recall that a perfect ROC curve is a step function, meaning TPR is always one, while FPR linearly increases when the feature parameter is increased. We observe that the ROC curve for the second feature is perfect while that for the first feature is close to perfect. Therefore, these two features are excellent in distinguishing healthy subjects from patients with CHF. For ease of comparison with other metrics to be discussed in the next section, in Table 2, we have listed TPR values corresponding to five cases of FPR, $\leq 5\%$, $\leq 10\%$, $\leq 20\%$, $\leq 30\%$, and $\leq 40\%$.

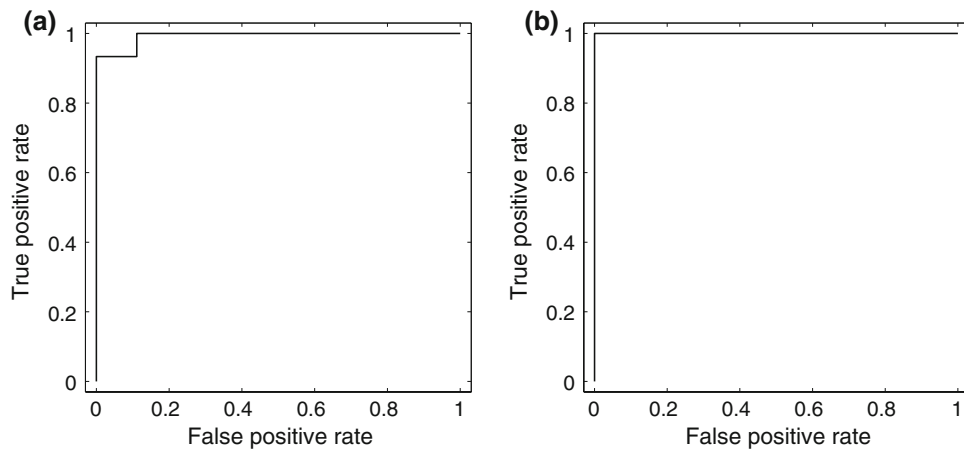


FIGURE 8. Receiver operating characteristic (ROC) curves using the two features (one is to characterize how well the linear relation between $\lambda(\epsilon)$ and $\ln \epsilon$ is defined, and the other to characterize how well the characteristic scale ϵ_∞ is defined, see “HRV Analysis by SDLE” section for more details) derived from the SDLE (in \log_{10} scale) in distinguishing healthy subjects from patients with CHF: the value of feature 1(a) and feature 2(b) decrease from -0.75 to about -1.75 and from 0.40 to about -0.50 when FPR increases from 0 to 1.

TABLE 2. Evaluation of the effectiveness of different metrics for distinguishing healthy subjects from patients with CHF.

FPR, %	SDLE				
	Feature 1 TPR (threshold)	Feature 2 TPR (threshold)	H parameter TPR (threshold)	Sample entropy TPR (threshold)	Multiscale entropy TPR (threshold)
≤ 5	93.33% (-0.86)	100.00% (0.39)	46.67% (0.20)	5.56% (1.82)	66.67% (1.30)
≤ 10	93.33% (-0.91)	100.00% (0.38)	53.33% (0.16)	5.56% (1.76)	83.33% (1.19)
≤ 20	100.00% (-1.13)	100.00% (0.32)	66.67% (0.15)	38.89% (1.19)	94.44% (1.00)
≤ 30	100.00% (-1.20)	100.00% (0.25)	80.00% (0.12)	50.00% (1.17)	94.44% (0.88)
≤ 40	100.00% (-1.26)	100.00% (0.17)	80.00% (0.10)	88.89% (0.96)	94.44% (0.81)

The threshold values for the parameters corresponding to the given TPR and FPR are given within the parentheses.

DISTINGUISHING HEALTHY SUBJECTS FROM PATIENTS WITH CHF USING OTHER COMPLEXITY MEASURES

To evaluate the effectiveness of distinguishing healthy subjects from patients with CHF using features derived from the SDLE, it is important to compare their performance with those based on other complexity measures. For this purpose, we again focus on the set of HRV with 18 healthy and 15 CHF subjects, and consider three complexity measures, the Hurst parameter, the sample entropy,²⁸ and the multiscale entropy (MSE),³ which are among the most promising complexity measures proposed for the analysis of HRV.

Fractal Analysis of HRV Using the Hurst Parameter

One of the simplest multiscale analyses is the structure-function based multifractal formulation.^{4,8} It is especially convenient for the study of the ubiquitous $1/f$ noise, which is among the earliest and most elegant models for HRV.²⁰ In the literature, HRV data, denoted as $x(n)$, $n = 1, \dots$, are considered “random walk” processes, and one examines whether the following scaling-law holds or not,

$$F^{(q)}(m) = \langle |x(i+m) - x(i)|^q \rangle^{1/q} \sim m^{H(q)}, \quad (13)$$

where $H(q)$ is a function of real value q , and the average is taken over all possible pairs of $(x(i+m), x(i))$. Large positive and negative q values emphasize large and small differences in $x(n)$, respectively. When the scaling laws described by Eq. (13) hold, the process under investigation is said to be a fractal process. Furthermore, if $H(q)$ is not a constant,

the process is a multifractal; otherwise, it is a monofractal. The case of $q = 2$ is of special interest. It characterizes the correlation structure of the dataset. In fact, when Eq. (13) holds, the autocorrelation $r(k)$ for the “increment” process, defined as $w(i) = x(i+1) - x(i)$, decays as a power-law, $r(k) \sim k^{2H(2)-2}$, as $k \rightarrow \infty$, while the PSD for $x(n)$, $n = 1, \dots$ is $E_x(f) \sim 1/f^{2H(2)+1}$. $H(2)$ is often called the Hurst parameter, and simply denoted as H . In parallel, $F^{(2)}(m)$ is often written as $F(m)$, and the method based on Eq. (13) is called fluctuation analysis (FA).

We estimated the Hurst parameter from the same HRV datasets analyzed by the SDLE. One typical $\log_2 F(m)$ vs. $\log_2 m$ curve of HRV data for a normal subject is shown in Fig. 9a. We observe that the power-law relation is not well defined. This is because the data sometimes appear oscillatory, as shown in Figs. 1b and 1d. If we nevertheless fit a straight line to the plot in Fig. 9a, we find that the Hurst parameter H for the healthy subjects is smaller than 0.5 and generally smaller than those for the patients with CHF, consistent with published results.^{1,18,23} However, the accuracy of H as a discriminator for separating healthy subjects from patients with CHF is not very high. This is shown by the ROC curve in Fig. 9b and the TPR values in Table 2.

There are many ways to estimate the Hurst parameter, including variance-time plot, detrended FA, and wavelet multiresolution analysis (for an in depth discussion of these and other methods, we refer to Gao *et al.*^{4,8}). While they are equivalent when characterizing simulated random fractal processes, some are more effective than others in characterizing real world data. For HRV data, however, we have found that H values estimated by different methods are

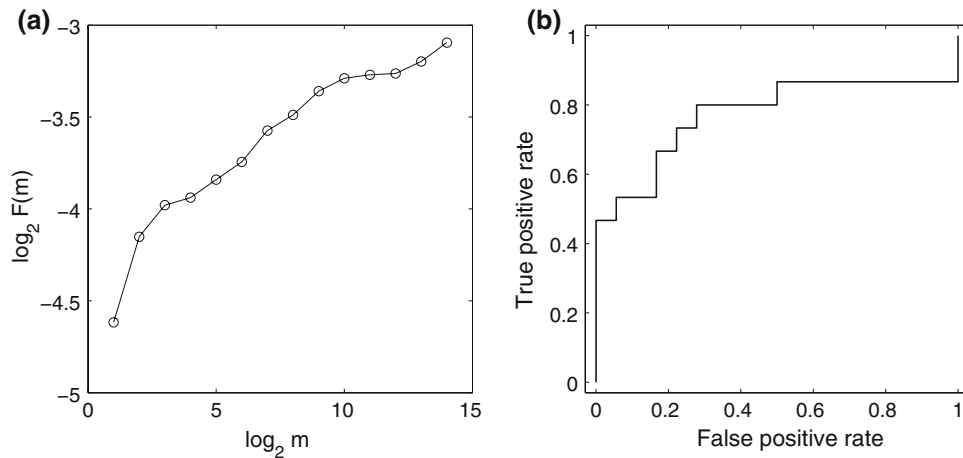


FIGURE 9. (a) A typical $\log_2 F(m)$ vs. $\log_2 m$ curve for HRV. (b) The ROC curve using the Hurst parameter in distinguishing healthy subjects from patients with CHF. The Hurst parameter decreases from 0.22 to about 0.02 when TPR and FPR increase from 0.27 to 1 and from 0 to 1, respectively.

always consistent with those estimated by FA. Therefore, the low accuracy of using H to distinguish healthy subjects from patients with CHF suggests that raw HRV data are not ideally fractal processes, but are highly nonstationary, just as we have observed in Fig. 1.

Entropy Analysis

Entropy characterizes creation of information in a dynamical system. For a chaotic system, one of the most important measures is the Kolmogorov entropy. For a given finite time series, to get better statistics, the Kolmogorov entropy is often estimated through its tight-lower bound, the correlation entropy $K_2(\epsilon)$, by using Grassberger–Procaccia’s algorithm^{14,15}:

$$K_2(\epsilon) = \lim_{m \rightarrow \infty} \frac{\ln C^{(m)}(\epsilon) - \ln C^{(m+1)}(\epsilon)}{mL\delta t}, \quad (14)$$

where δt is the sampling time, $C^{(m)}(\epsilon)$ is the correlation integral based on the m -dimensional reconstructed vectors V_i and V_j ,

$$C^{(m)}(\epsilon) = \lim_{N_v \rightarrow \infty} \frac{2}{N_v(N_v - 1)} \sum_{i=1}^{N_v-1} \sum_{j=i+1}^{N_v} \Theta(\epsilon - \|V_i - V_j\|), \quad (15)$$

where N is the length of the original data, $N_v = N - (m - 1)L$ is the number of reconstructed vectors, $\Theta(y)$ is the Heaviside function (1 if $y \geq 0$ and 0 if $y < 0$). $C^{(m+1)}(\epsilon)$ can be computed similarly based on the $(m + 1)$ -dimensional reconstructed vectors. When one evaluates $K_2(\epsilon)$ at a finite fixed scale $\hat{\epsilon}$ (say 15% or 20% of the standard deviation of the data), one obtains the sample entropy S_e .²⁸

Next we explain MSE analysis.³ Given a time series $X = \{x_t; t = 1, 2, \dots\}$, one constructs a new time series

$$X^{(b_s)} = \{x_t^{(b_s)} : t = 1, 2, 3, \dots\}, \quad b_s = 1, 2, 3, \dots,$$

by averaging the original series X over nonoverlapping blocks of size b_s ,

$$x_t^{(b_s)} = (x_{tb_s-b_s+1} + \dots + x_{tb_s})/b_s, \quad t \geq 1. \quad (16)$$

Note b_s is often called the coarse-graining parameter. MSE involves calculating the sample entropy from the coarse-grained time series $X^{(b_s)}$, where $b_s = 1$ corresponds to the original time series.

Following Costa *et al.*,³ we have estimated the sample entropy at $\hat{\epsilon} = 15\%$ of the standard deviation of the original HRV data and the MSE with the smoothing scale b_s ranging from 1 to 20. The ROC curve for the sample entropy is shown in Fig. 10a, while that for the MSE at $b_s = 10$ is shown in Fig. 10b (See also a few TPR values listed in Table 2). Note that the ROC curves for the MSE at other b_s values are either similar to Fig. 10b or in between Figs. 10a and 10b. We observe that the accuracy of sample entropy as a discriminator for separating healthy subjects from patient with CHF is as bad as (or even worse than) that of the Hurst parameter. The MSE has major improvements over the Hurst parameter and the sample entropy. However, it is still much worse than the two features derived from SDLE.

CONCLUDING DISCUSSIONS

To shed new light on determining whether HRV is chaotic or stochastic, as well as deriving new metrics

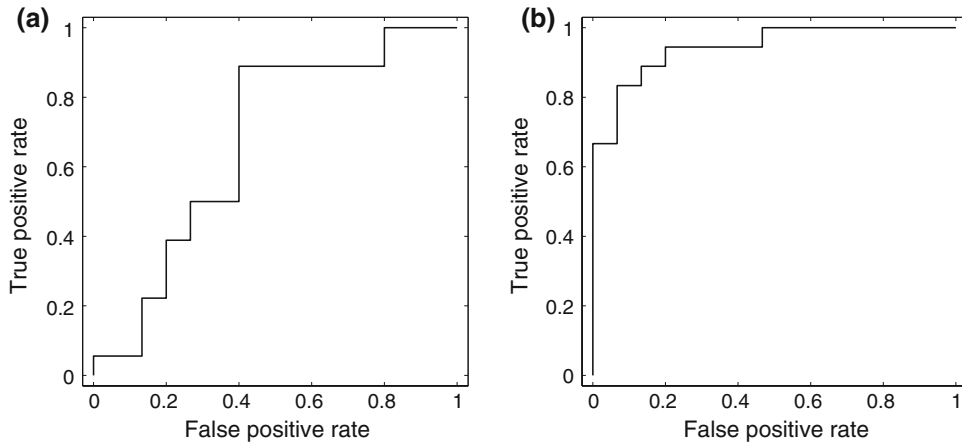


FIGURE 10. The ROC curves using the sample entropy (a) and multiscale entropy (b) in distinguishing healthy subjects from patients with CHF. In (a), the value of the sample entropy decreases from 1.85 to about 0.35 when TPR and FPR increase from 0.06 to 1 and from 0 to 1, respectively; in (b), the value of the decreases from 1.48 to 0.48 when TPR and FPR increase from 0.5 to 1 and from 0 to 1, respectively.

that can effectively distinguish healthy subjects from patients with cardiac disease, in this paper, we have employed SDLE to characterize HRV. We have not observed the chaotic scaling described by Eq. (9) on any significant scale ranges from any of the HRV datasets analyzed here. Instead, we have found that the dynamics in HRV of healthy subjects are characterized by scalings of Eq. (10) and (12) on different scale ranges, the dynamics of HRV in CHF patients are mostly like $1/f$ processes, while that in AF patients are like white noise. While none of the three types of HRV is low-dimensional, the dimension increases from normal to CHF to AF.

We have also considered the important problem of distinguishing healthy subjects from patients with CHF through HRV analysis. We have derived two features from the SDLE, one is to characterize how well the linear relation between $\lambda(\epsilon)$ and $\ln \epsilon$ is defined, and the other to characterize how well the characteristic scale ϵ_∞ is defined. We have shown that both features are very effective in achieving this goal. The same task is evaluated using other complexity measures, including the Hurst parameter, the sample entropy, and the MSE. We have shown that the sample entropy and the Hurst parameter are very in-effective. Although MSE is a major improvement over the sample entropy and the Hurst parameter, it is still much less effective than the two features derived from the SDLE.

It is important to understand the relative effectiveness of these complexity measures in separating healthy subjects from patients with CHF. While the in-effectiveness of the Hurst parameter and the sample entropy in distinguishing healthy subjects from patients with CHF is, to a large extent, due to the nonstationarity in the HRV data, it also signifies that the HRV dynamics are neither entirely random nor simply chaotic. Such a picture is consistent with the scaling law of the SDLE described by Eq. (10) for healthy subjects: the HRV dynamics for normal subjects are like noisy dynamics. The MSE improves on the sample entropy, because it contains an additional parameter, the scale b_s for smoothing, and therefore, provides a better characterization of HRV dynamics. However, it is still not as effective as the two features derived from the SDLE, because the SDLE can classify all the known types of complex time series encountered so far, while MSE cannot.

Finally, we comment on how SDLE may deal with nonstationarity and its potential limitations. In Gao *et al.*⁴ and Hu *et al.*,¹⁶ we have shown that when a chaotic or fractal $1/f$ signal is mixed with an oscillatory signal, the positive part of SDLE will not be affected much. This means SDLE can readily deal with certain types of nonstationarity. The fact that SDLE can be

readily computed from raw, rather than filtered HRV data, and that the γ parameter is very insensitive to the data length (Fig. 4) re-affirms this. Another feature related to nonstationarity is to detect dynamical changes in complex systems, such as to detect epileptic seizures from EEG recordings. This may be achieved by partitioning (long) dataset into short segments, either with or without overlap, and computing SDLE from each short segment. When the underlying dynamics change, the metrics derived from the SDLE may indicate the dynamical transitions. While these are all attractive features of SDLE, we would like to caution that when little is known about a dataset, improper choice of embedding parameters, or shortness of a dataset may prevent one from observing the underlying scaling relations. In such situations, a safe rule of thumb would be to systematically vary the embedding parameters. However, if the shortness of a dataset is the major problem, then one has to try other methods such as random fractal theory-based approaches.⁴

ACKNOWLEDGMENTS

The authors are grateful for reviewers' many constructive comments, which have improved the paper considerably. This work is partially supported by NSF grants CMMI-0825311 and 0826119.

REFERENCES

- ¹Ashkenazy, Y., P. Ivanov, S. Havlin, C. Peng, A. Goldberger, and H. Stanley. Magnitude and sign correlations in heart-beat fluctuations. *Phys. Rev. Lett.* 86:1900–1903, 2001.
- ²Bigger, J., R. Steinman, L. Rolnitzky, J. Fleiss, P. Albrecht, and R. Cohen. Power law behavior of rr-interval variability in healthy middle-aged persons, patients with recent acute myocardial infarction, and patients with heart transplants. *Circulation* 93:2142–2151, 1996.
- ³Costa, M., A. Goldberger, and C. Peng. Multiscale entropy analysis of biological signals. *Phys. Rev. E* 71:021–906, 2005.
- ⁴Gao, J., Y. Cao, W. Tung, and J. Hu. *Multiscale Analysis of Complex Time Series—Integration of Chaos and Random Fractal Theory, and Beyond*. Wiley, NJ, 2007.
- ⁵Gao, J., C. Chen, S. Hwang, and J. Liu. Noise-induced chaos. *Int. J. Mod. Phys. B* 13:3283–3305, 1999.
- ⁶Gao, J., S. Hwang, and J. Liu. When can noise induce chaos? *Phys. Rev. Lett.* 82:1132–1135, 1999.
- ⁷Gao, J., J. Hu, W. Tung, and Y. Cao. Distinguishing chaos from noise by scale-dependent lyapunov exponent. *Phys. Rev. E* 74:066204, 2006.
- ⁸Gao, J., J. Hu, W. Tung, Y. Cao, N. Sarshar, and V. Roychowdhury. Assessment of long range correlation in

- time series: how to avoid pitfalls. *Phys. Rev. E* 73:016117, 2000.
- ⁹Gao, J., W. Tung, and J. Hu. Quantifying dynamical predictability: the pseudo-ensemble approach. *Chi. Ann. Math. Ser. B* 30:569–588, 2009.
- ¹⁰Gao, J., and Z. Zheng. Local exponential divergence plot and optimal embedding of a chaotic time series. *Phys. Lett. A* 181:153–158, 1993.
- ¹¹Gao, J., and Z. Zheng. Direct dynamical test for deterministic chaos. *Europhys. Lett.* 25:485–490, 1998.
- ¹²Gao, J., and Z. Zheng. Direct dynamical test for deterministic chaos and optimal embedding of a chaotic time series. *Phys. Rev. E* 49:3807–3814, 1994.
- ¹³Gaspard, P., and X. Wang. Noise, chaos, and (ϵ, τ) -entropy per unit time. *Phys. Rep.* 235:291–343, 1993.
- ¹⁴Grassberger, P., and I. Procaccia. Characterization of strange attractors. *Phys. Rev. Lett.* 50:346–349, 1983.
- ¹⁵Grassberger, P., and I. Procaccia. Estimation of the kolmogorov entropy from a chaotic signal. *Phys. Rev. A* 28:2591–2593, 1983.
- ¹⁶Hu, J., J. Gao, and W. Tung. Characterizing heart rate variability by scale-dependent lyapunov exponent. *Chaos* 19:028506, 2009.
- ¹⁷Hwang, K., J. Gao, and J. Liu. Noise-induced chaos in an optically injected semiconductor laser. *Phys. Rev. E* 61:5162–5170, 2000.
- ¹⁸Ivanov, P., L. Amaral, A. Goldberger, S. Havlin, M. Rosenblum, Z. Struzik, and H. Stanley. Multifractality in human heartbeat dynamics. *Nature* 399:461–465, 1999.
- ¹⁹Kanters, J., N. Holstein-Rathlou, and E. Agner. Lack of evidence for low-dimensional chaos in heart rate variability. *J. Cardiovasc. Electrophysiol.* 5:591–601, 1994.
- ²⁰Kobayashi, M., and T. Musha. 1/f fluctuation of heart beat period. *IEEE Trans. Biomed. Eng.* 29:456–457, 1982.
- ²¹Osaka, M., K. Chon, and R. Cohen. Distinguishing cardiac randomness from chaos. *J. Cardiovasc. Electrophysiol.* 6:441–442, 1995.
- ²²Packard, N., J. Crutchfield, J. Farmer, and R. Shaw. Gemometry from time-series. *Phys. Rev. Lett.* 45:712–716, 1980.
- ²³Peng, C., J. Mietus, J. Hausdorff, S. Havlin, H. Stanley, and A. Goldberger. Long-range anticorrelations and non-gaussian behavior of the heartbeat. *Phys. Rev. Lett.* 70:1343–1346, 1993.
- ²⁴Peng, C., S. Havlin, H. Stanley, and A. Goldberger. Quantification of scaling exponents and crossover phenomena in nonstationary heartbeat time series. *Chaos* 5:82–87, 1995.
- ²⁵Pincus, S., and R. Viscarello. Approximate entropy: a regularity statistic for fetal heart rate analysis. *Obst. Gynecol.* 79:249–255, 1992.
- ²⁶Poon, C. The chaos about heart rate chaos. *J. Cardiovasc. Electrophysiol.* 11:235–236, 2000.
- ²⁷Poon, C., and C. Merrill. Decrease of cardiac chaos in congestive heart failure. *Nature* 389:492–495, 1997.
- ²⁸Richman, J., and J. Moorman. Physiological time-series analysis using approximate entropy and sample entropy. *Am. J. Physiol. Heart Circ. Physiol.* 278:H2039–H2049, 2000.
- ²⁹Sauer, T., J. Yorke, and M. Casdagli. Embedology. *J. Stat. Phys.* 65:579–616, 1991.
- ³⁰Saul, J., P. Albrecht, R. Berger, and R. Cohen. Analysis of long-term heart rate variability: methods, 1/f scaling and implications. *Comput. Cardiol.* 14:419–422, 1988.
- ³¹Takens, F. Detecting strange attractors in turbulence. In: *Dynamical Systems and Turbulence, Lecture Notes in Mathematics* 898, edited by D. A. Rand and L. S. Young, Springer-Verlag, 366 p, 1981.
- ³²Task Force of the European Society of Cardiology and the North American Society of Pacing and Electrophysiology. Heart rate variability: standards of measurement, physiological interpretation, and clinical use. *Circulation* 93:1043–1065, 1996.
- ³³Wolf, A., J. Swift, H. Swinney, and J. Vastano. Determining lyapunov exponents from a time series. *Phys. D* 16:285, 1985.
- ³⁴Wu, G., N. Arzeno, L. Shen, D. Tang, D. Zheng, N. Zhao, D. Eckberg, and C. Poon. Chaotic signatures of heart beat variability and its power spectrum in health, aging and heart failure. *PLoS ONE* 4:e4323, 2009.